Supporting Information

Stabilizing CuTCNQ Cathodes in Sulfide-Based All-Solid-State Organic Lithium Batteries via a Fluoroiodinated Molecular Modifier

Wenwen Deng[a,b*], Ying Zhou[c], Yuanyuan Quan[c], Yuhang Guo[a], Tianxiang Wei[a], Zhong Jin[b*]

a School of Materials Science and Engineering, Anhui University, 230601 Hefei, Anhui, PR China

b State Key Laboratory of Coordination Chemistry, MOE Key Laboratory of Mesoscopic Chemistry, MOE Key Laboratory of High Performance Polymer Materials and Technology, Jiangsu Key Laboratory of Clean Energy Catalysis and Intelligent Green Chemical Engineering, Suzhou Key Laboratory of Green Intelligent Manufacturing of New Energy Materials and Devices, Tianchang New Materials and Energy Technologies Research Center, Institute of Green Chemistry and Engineering, School of Chemistry and Chemical Engineering, Nanjing University, Nanjing, Jiangsu 210023, China

c School of Material Science and Engineering, Suzhou University of Science and Technology, Suzhou 215000, China

Experimental Section:

Synthesis of CuTCNQ (I Phase): CuTCNQ (I phase) was synthesized following a reported procedure. Equimolar amounts of CuI and TCNQ were separately dissolved in anhydrous acetonitrile inside an Ar-filled glovebox. The two solutions were then mixed and stirred vigorously for 3 min at room temperature. Deep-blue crystals precipitated immediately, which were collected by vacuum filtration and thoroughly washed with acetonitrile until the filtrate became pale green. The resulting solid was dried under vacuum overnight to obtain phase-pure CuTCNQ.

Preparation of CuTCNQ-x Composites: CuTCNQ-x (x = 2, 3, 4, 5) composites were synthesized via a chemical reaction between CuTCNQ and different amounts of $C_6F_{13}I$. The parameter x represents the volume ratio of $C_6F_{13}I$ (μL) to the mass of CuTCNQ (mg). The sealed reaction mixtures were heated at 150 °C for 6 h under an inert atmosphere, yielding CuTCNQ@$C_6F_{13}I$ composite denoted as CuTCNQ-2, CuTCNQ-3, CuTCNQ-4, and CuTCNQ-5.

Calculation: Density functional theory (DFT) calculations were conducted using the Vienna ab initio simulation package (VASP)[1]. The Perdew-Burke-Ernzerhof (PBE) functional with the generalized gradient approximation was used to describe the electronic exchange and correlation[2]. The projector augmented-wave (PAW) method was used to treat the interaction between the valence electrons and ionic cores[3]. K-points were set at 1 x 2 x 1 on a Monkhorst-Pack grid, and a cut-off energy of 450 eV was employed. Gaussian smearing scheme with a small SIGMA of 0.05 was employed. All DFT calculations were performed with the goal of minimizing residual forces until the convergence criterion of 0.02 eV/Å was reached. For vdW-dispersion energy-correction, the DFT-D3 method proposed by Grimme et al[4] was utilized.

Fabrication of Composite Cathodes: In an Ar-filled glovebox (H_2O < 0.01 ppm, O_2 < 0.01 ppm), CuTCNQ-x, LPSCl, and Super P were weighed according to different ratios to obtain a total mass of 100 mg. The mixture was manually ground in an agate mortar for 20 min, followed by ball milling in a 5 mL stainless-steel jar for 1 h under Ar atmosphere. The resulting powders were collected and stored in the glovebox for subsequent cell assembly.

Cell Assembly and Electrochemical Measurements: All-solid-state cells were assembled in PEEK–Ti alloy cell housings with a 10 mm diameter. A 370 MPa pressure was first applied for 5 min to compact 80 mg of LPSCl powder. Subsequently, 5–6 mg of the composite cathode was placed on one side of the electrolyte and pressed again at 370 MPa for 5 min. A lithium metal foil (10 mm diameter) was placed on the opposite side and pressed at 50 MPa for 3 min. The assembled cells were secured with screws and rested for 8 h prior to testing to achieve interfacial equilibrium. The applied pressure during battery testing was approximately 20 MPa.

Galvanostatic charge/discharge cycling was performed using a LAND multi-channel battery testing system. The CuTCNQ-based all-solid-state organic batteries were cycled between 1.6 V and 3.6 V. The theoretical specific capacity was set to 200 mAh g^{-1} (1 C), and rate performances were evaluated at current densities from 0.1 C to 2 C.

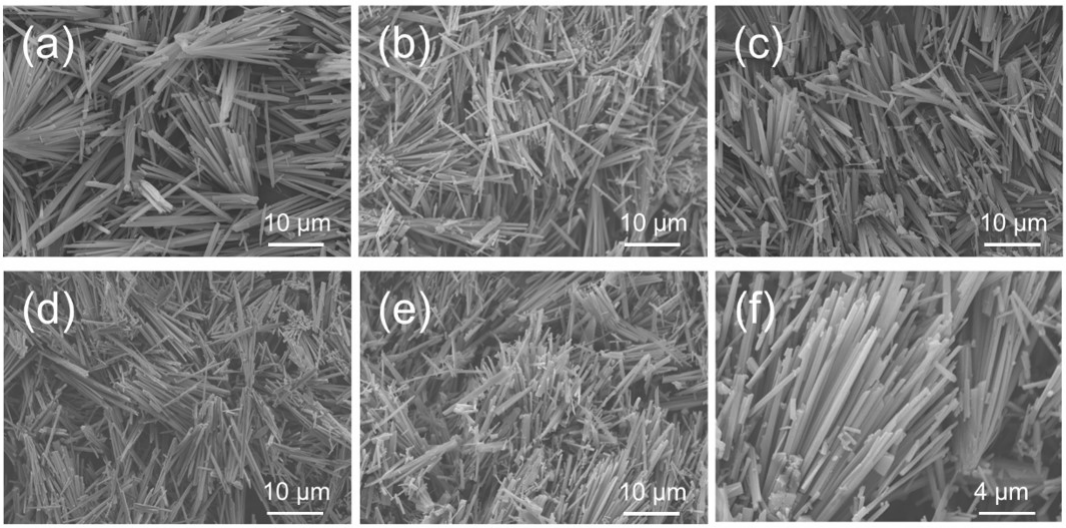

Figure S1 SEM images of CuTCNQ electrodes before and after treatment with different ratios of $C_6F_{13}I$: (a) pristine CuTCNQ, (b) CuTCNQ-2, (c) CuTCNQ-3, (d) CuTCNQ-4, (e) CuTCNQ-5, and (f) a magnified SEM image of CuTCNQ-4.

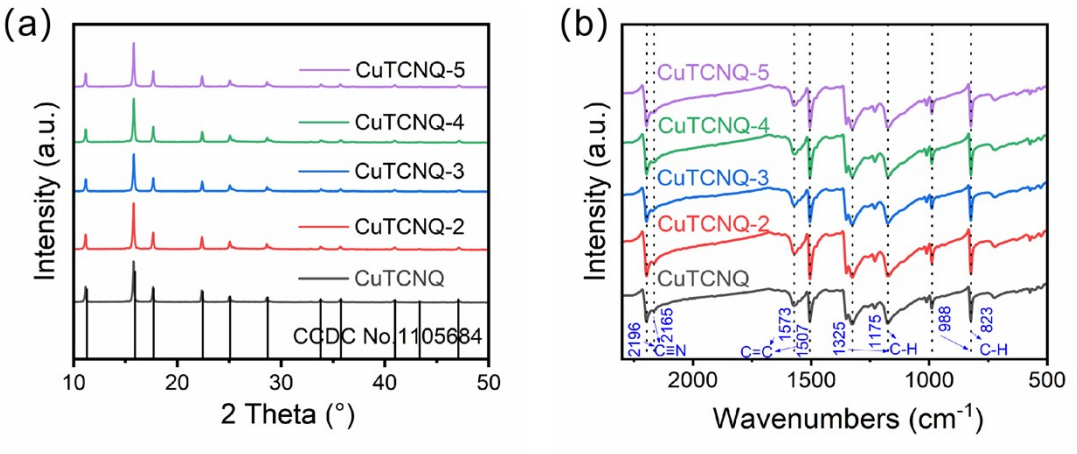

Figure S2 (a) X-ray diffraction (XRD) patterns of pristine CuTCNQ and CuTCNQ-x (x = 2–5) samples, where all diffraction peaks match well with the CuTCNQ-I phase (CCDC No. 1105884); (b) Fourier-transform infrared (FT-IR) spectra of CuTCNQ and CuTCNQ-x samples.

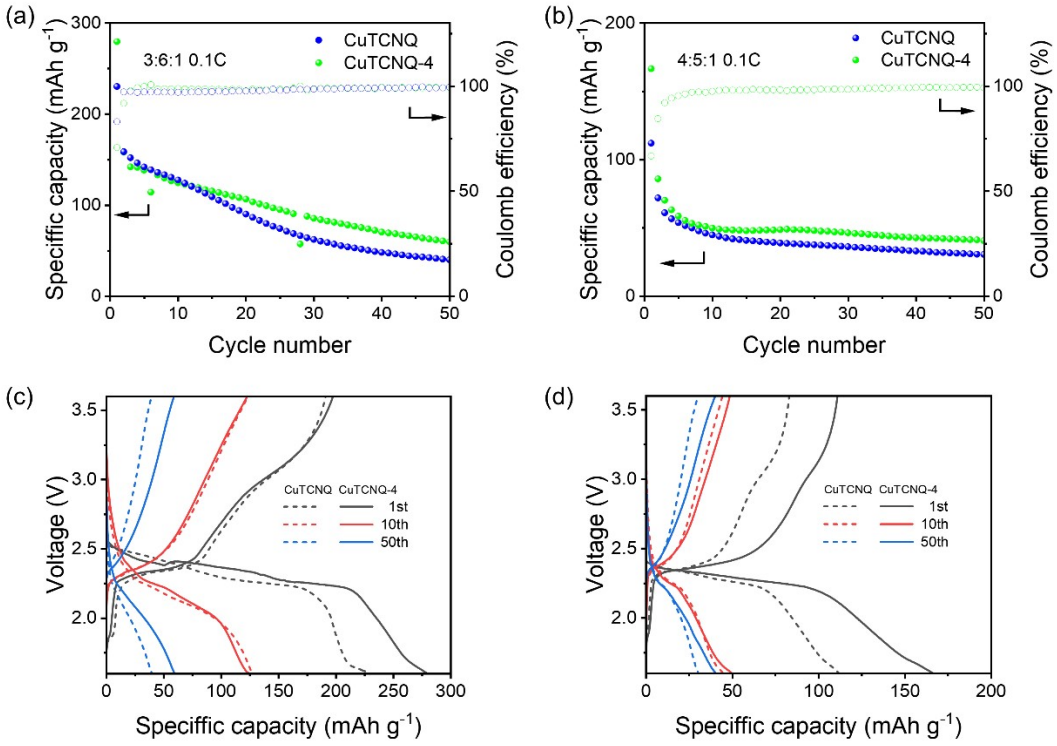

Figure S3 Electrochemical performance of CuTCNQ and CuTCNQ-4 at 0.1 C with different active material ratios: (a) 3:6:1(mass loading: 2.4 mg cm^{-2}) and (b) 4:5:1(mass loading: 3.2 mg cm^{-2}); corresponding charge/discharge profiles for (c) 3:6:1 and (d) 4:5:1 configuration.

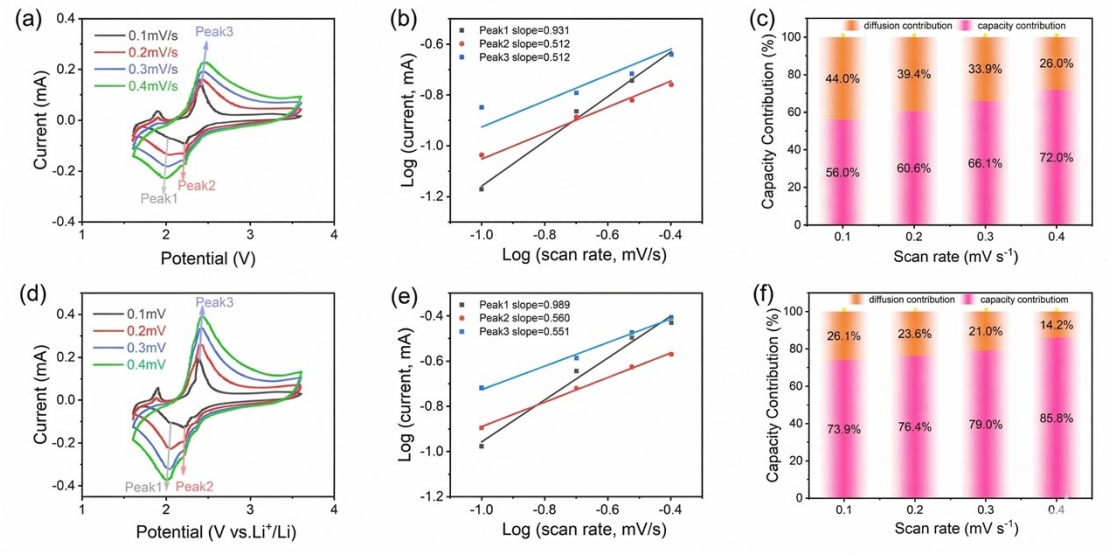

Figure S4 Cyclic voltammetry (CV) analyses of CuTCNQ and CuTCNQ-4 electrodes at 60 °C under various scan rates. (a, d) CV curves of CuTCNQ and CuTCNQ-4 recorded at scan rates from 0.1 to 0.4 mV s^{-1}. (b, e) Linear relationships between log (v) and log (i) for the corresponding redox peaks. (c, f) Calculated capacitive contributions at different scan rates.

As shown in **Figure S4a** and **S4d**, both electrodes exhibit one oxidation peak and two reduction peaks. At low scan rates, a distinct oxidation peak appears at lower potentials, which disappears as the scan rate increases—consistent with the charge/discharge profiles.

The relationship between the current (i) and scan rate (v) follows Equation (1): $i = av^b$, where the b-value reflects the charge-storage mechanism. Typically, $b = 1$ corresponds to a capacitive-controlled process, $b = 0.5$ to a diffusion-controlled process, and $0.5 < b < 1$ indicates mixed behavior. As shown in **Figure S4b** and **S4e**, the calculated b-values for CuTCNQ and CuTCNQ-4 are 0.93/0.51/0.51 and 0.99/0.56/0.55, respectively, suggesting that both electrodes exhibit a combination of ion-diffusion and pseudocapacitive behaviors.

The relative contributions of these two processes were further quantified using Equation (2): $i = k_1v + k_2v^{1/2}$, where k_1v and $k_2v^{1/2}$ represent the capacitive and diffusion-controlled currents, respectively. As illustrated in **Figure S4c** and **S4f,** the pseudocapacitive contribution of CuTCNQ increases from 56 % to 72 % as the scan rate rises from 0.1 mV s^{-1} to 0.4 mV s^{-1}, while that of CuTCNQ-4 increases from 73.9 % to 85.8 %. This enhancement at higher scan rates indicates a more prominent surface-controlled storage mechanism.

The higher pseudocapacitive fraction observed in CuTCNQ-4 can be attributed to structural modification induced by $C_6F_{13}I$ treatment, which optimizes charge distribution at the active material/electrolyte interface and facilitates faster charge transfer.

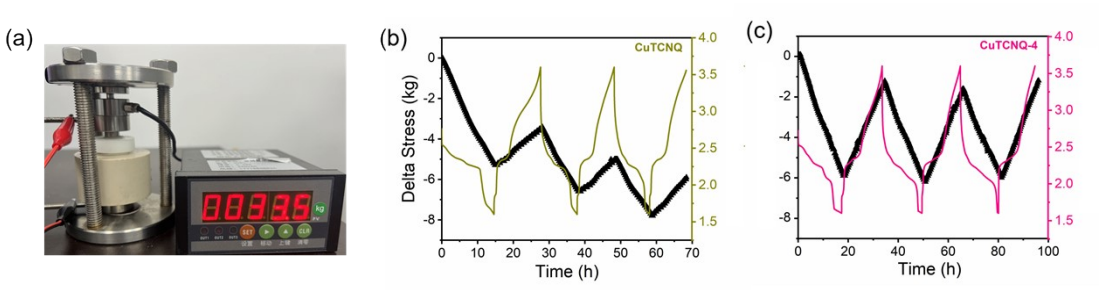

Figure S5 Operando stress analysis of Li/LPSC/CuTCNQ batteries.(a) Photograph of the operando pressure-monitoring setup for all-solid-state batteries. (b,c) Evolution of the voltage profiles (colored lines) and the corresponding Δ stress signals (black lines) of Li/LPSC/CuTCNQ and Li/LPSC/CuTCNQ-4 batteries during galvanostatic cycling, respectively.

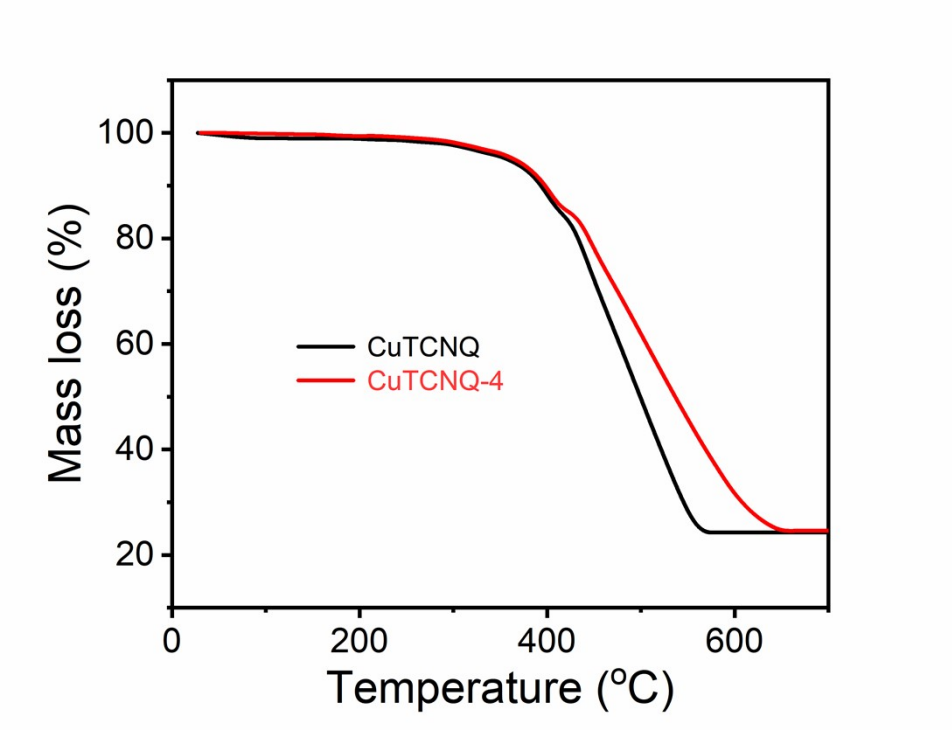

Figure S6 Thermogravimetric analysis (TGA) curves of pristine CuTCNQ and modified CuTCNQ-4 measured under an inert atmosphere.

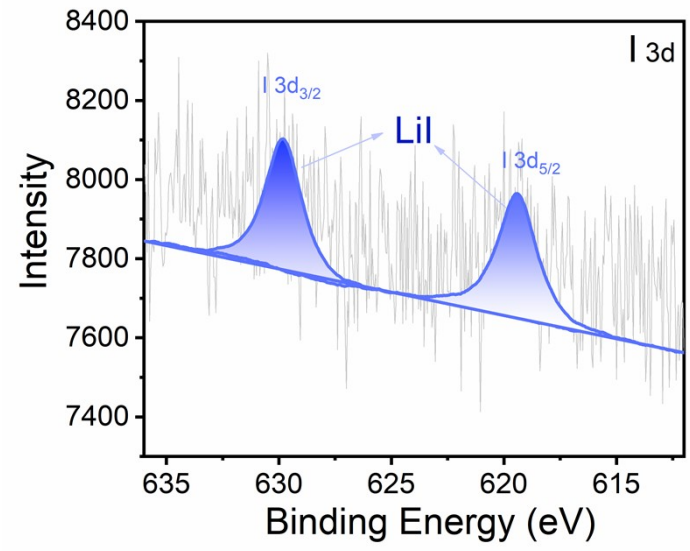

Figure S7 High-resolution X-ray photoelectron spectroscopy (XPS) spectrum of the I 3d in CuTCNQ-4 and LPSCl composite.

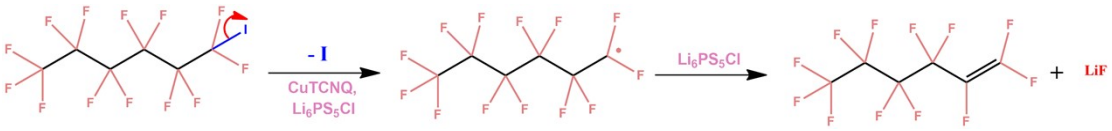

Scheme S1 Proposed reaction pathways of $C_6F_{13}I$ at the cathode side.

Supporting Information References

1. a) G. Kresse, J. Furthmüller, *Comput. Mater. Sci.* **1996**, *6*, 15-50; b) G. Kresse, J. Hafner, *Phys. Rev. B* **1993**, *48*, 13115-13118; c) G. Kresse, J. Hafner, *Phys. Rev. B* **1994**, *49*, 14251-14269.

2. J. P. Perdew, K. Burke, M. Ernzerhof, *Phys. Rev. Lett.* **1997**, *78*, 1396-1396.

3. P. Blöchl, *Phys. Rev. B* **1994**, 50, 17953.

4. S. Grimme, J. Antony, S. Ehrlich, and S. Krieg, J. Chem. Phys. **2010**, 132, 154104.